Heteroleptic Ru(II) cyclometalated complexes derived from benzimidazole-phenyl carbene ligands for dye-sensitized solar cells: experimental and theoretical approach

Tejaswi Jella,[a,b] Malladi Srikanth,[c] Yarasi Soujanya,[c] Surya Prakash Singh[a,b] Lingamallu Giribabu[a,b*] Ashraful Islam, [d*] Liyuan Han, [d] Idriss Bedja,[e] Ravindra Kumar Gupta[e]

[a,b]*Inorganic & Physical Chemistry Division, CSIR-Indian Institute of Chemical Technology,* and *CSIR-Network Institutes for Solar Energy (CSIR-NISE), Tarnaka,* and *CSIR-Network Institutes for Solar Energy (CSIR-NISE), Hyderabad-500007, (Telangana), India .Email: giribabu@iict.res.in. Phone: +91-40-27191724, Fax: +91-40-27160921 and Academy of Scientific and Innovative Research (AcSIR), New Delhi, India.*
[c]*Molecular Modelling Group, CSIR-Indian Institute of Chemical Technology, Hyderabad-500007, (Telangana), India.*
[d]*Photovoltaic Materials Unit, National Institute for Materials Science, 1-2-1 Sengen, Tsukuba, Ibaraki 305-0047, Japan.*
[e]CRC, Optometry Department, College of Applied Medical Sciences, King Saudi University, riyadh 11433, Saudi Arabia

	Table of Contents	Page No.

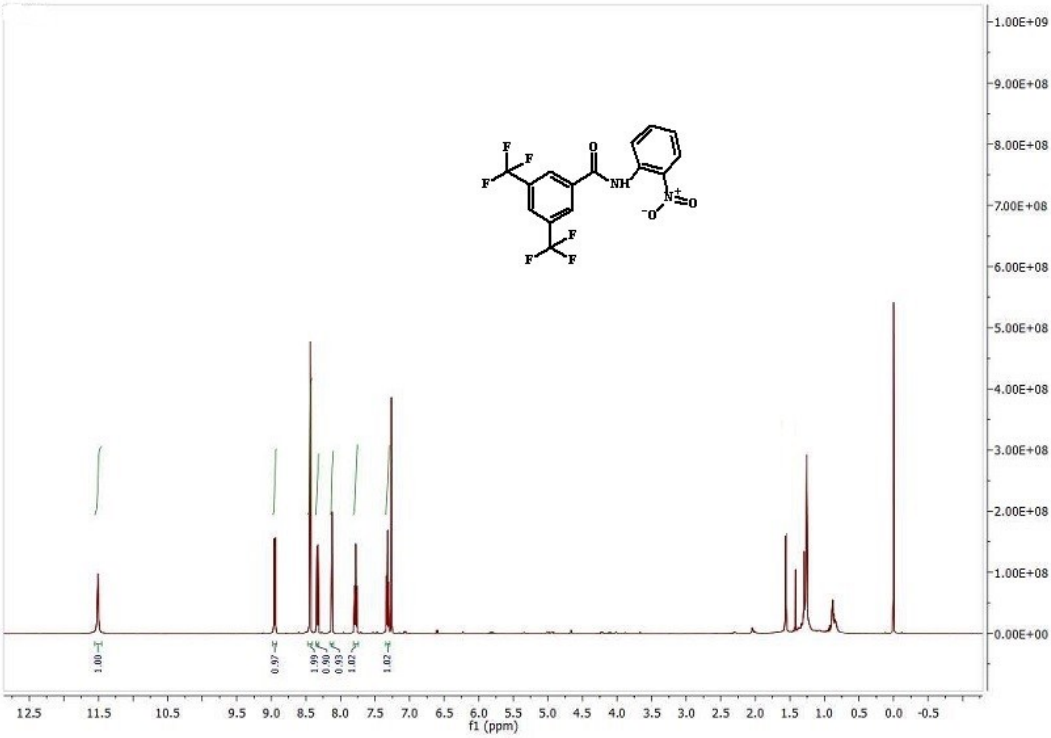

Fig. S1: ^{1}H NMR spectrum of **N-(2-nitrophenyl)-3,5-bis(trifluoromethyl)benzamide** (**1**) in $CDCl_3$.

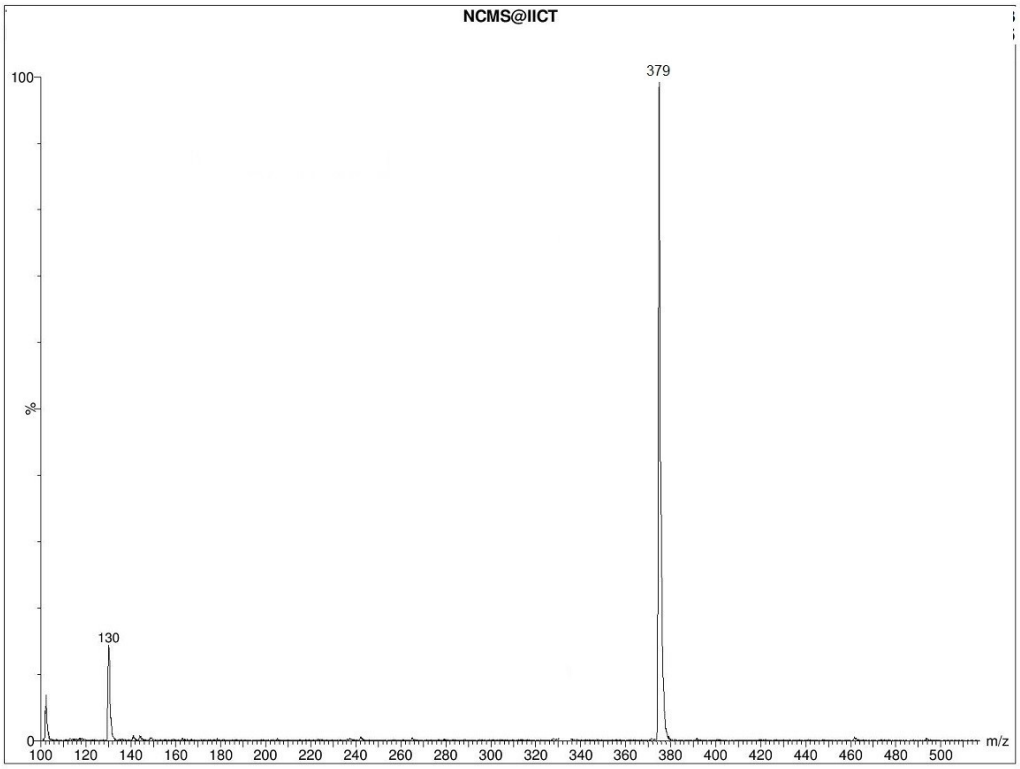

Fig. S2: ESI-MS spectrum of **N-(2-nitrophenyl)-3,5-bis(trifluoromethyl)benzamide** (**1**)

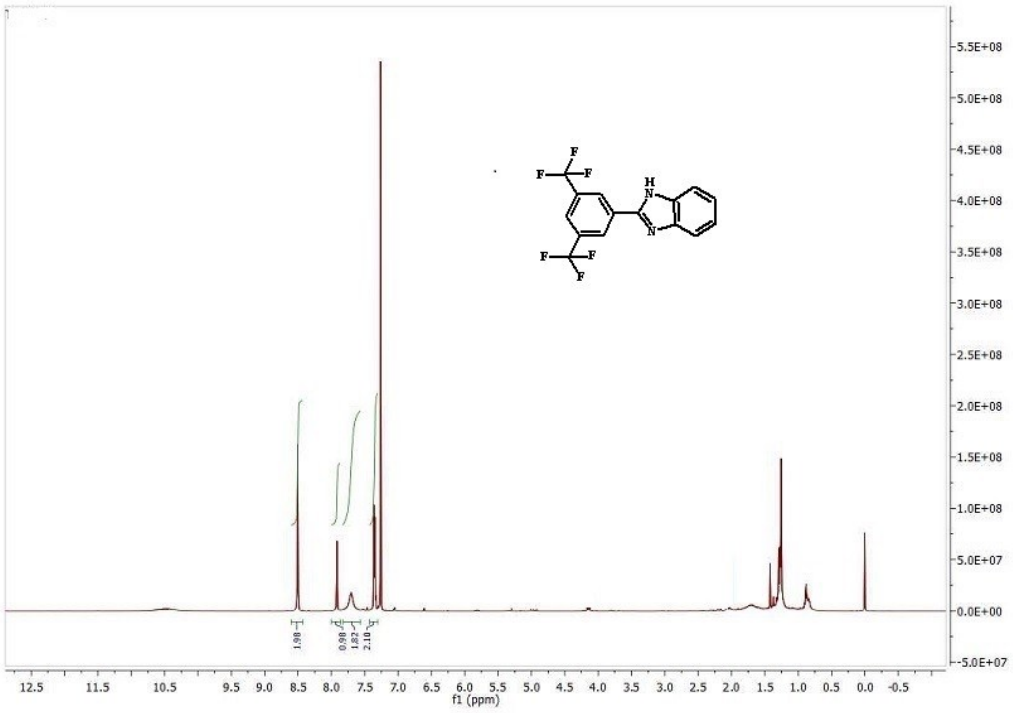

Fig. S3: ^{1}H NMR spectrum of 2-(3,5-bis(trifluoromethyl)phenyl)-1H-benzo[d]imidazole (**2**) in $CDCl_3$.

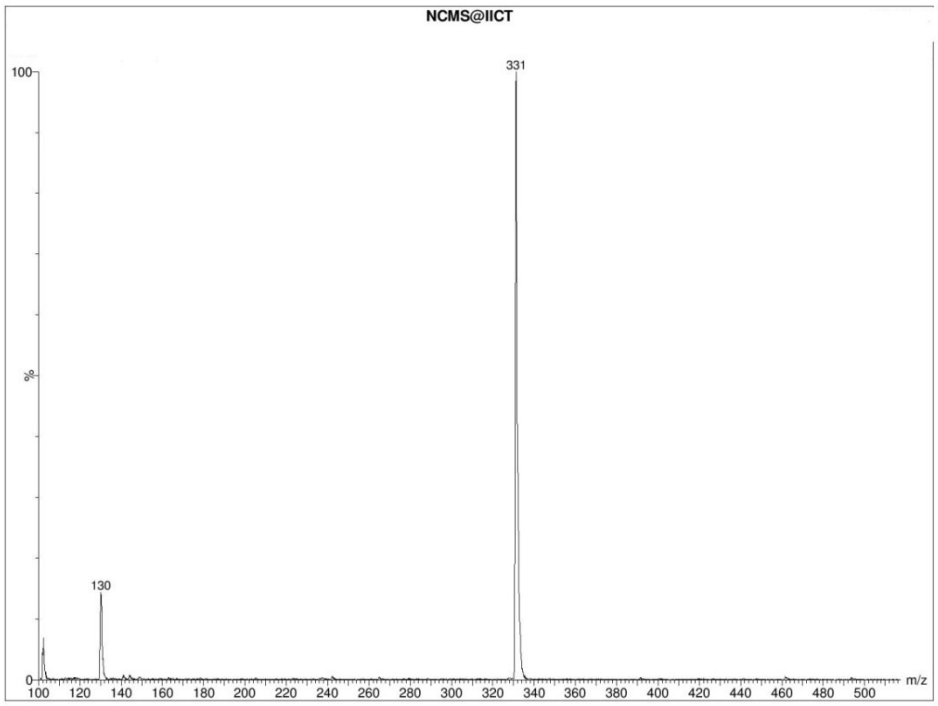

Fig. S4: ESI-Mass spectrum of 2-(3,5-bis(trifluoromethyl)phenyl)-1H-benzo[d]imidazole (**2**).

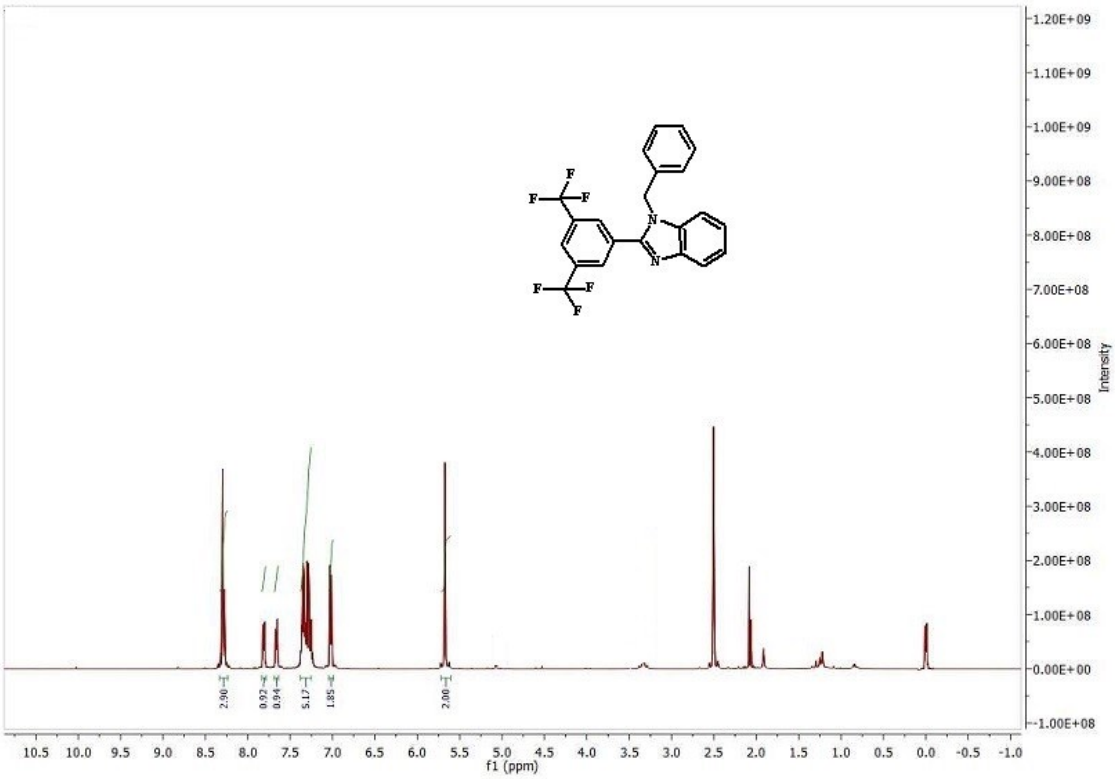

Fig. S5: ^{1}H NMR spectrum of 2-(3,5-bis(trifluoromethyl)phenyl)-1H-benzo[d]imidazole (**L1**) in $CDCl_3$.

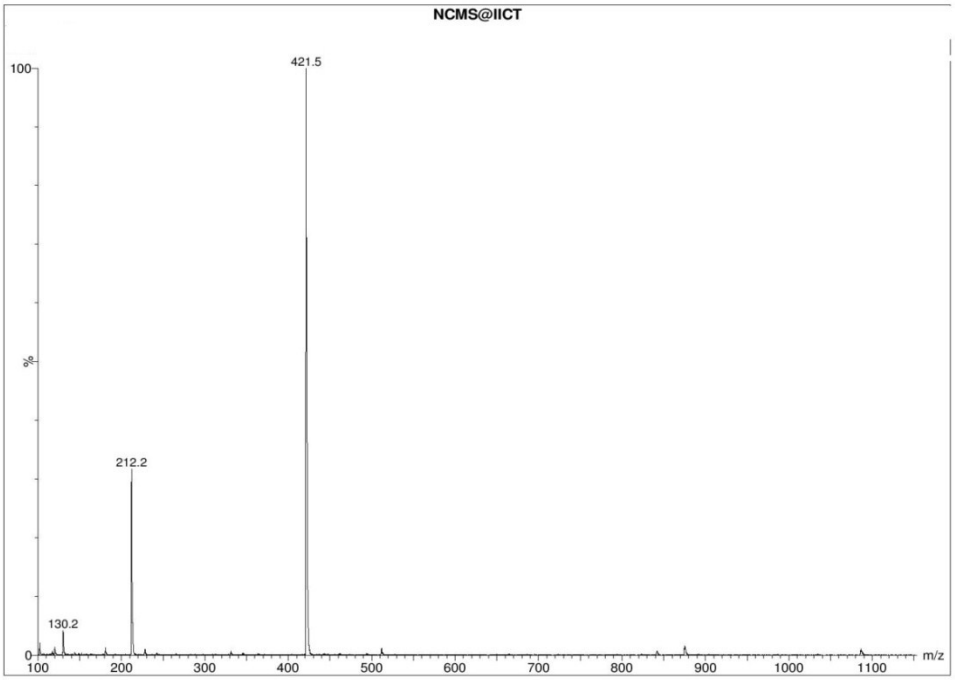

Fig. S6: ESI-Mass sepectrum of 2-(3,5-bis(trifluoromethyl)phenyl)-1H-benzo[d]imidazole (**L1**).

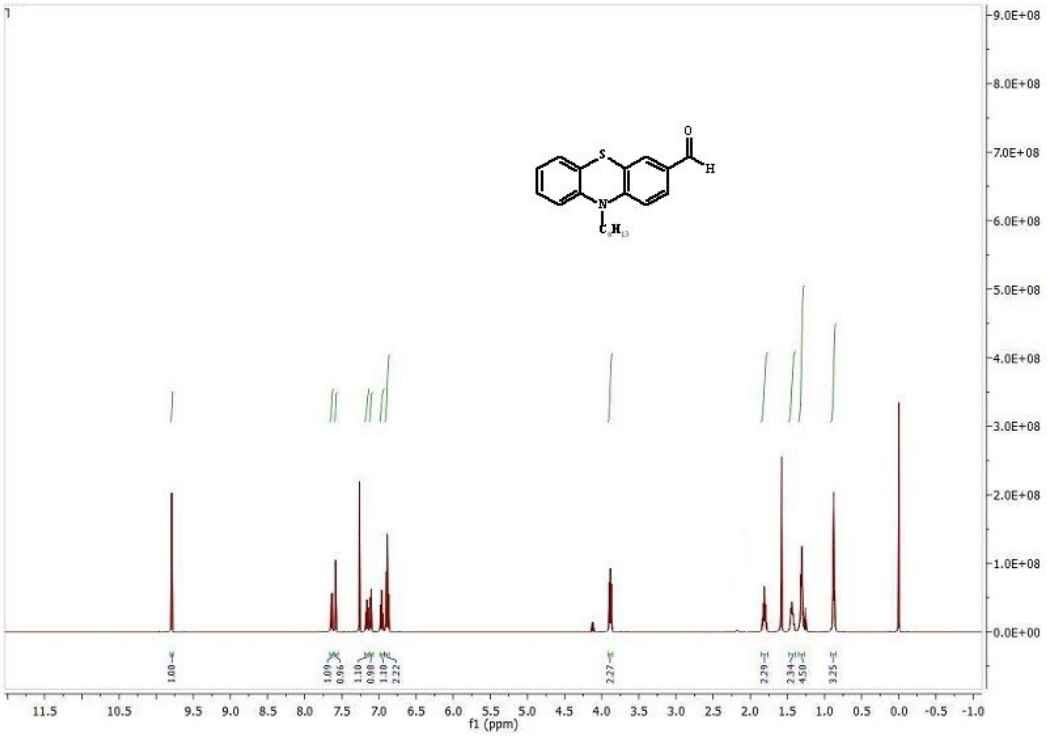

Fig. S7: ^{1}H NMR spectrum of **10-hexyl-penothiazine-3-carboxaldehyde** (**3**) in $CDCl_3$.

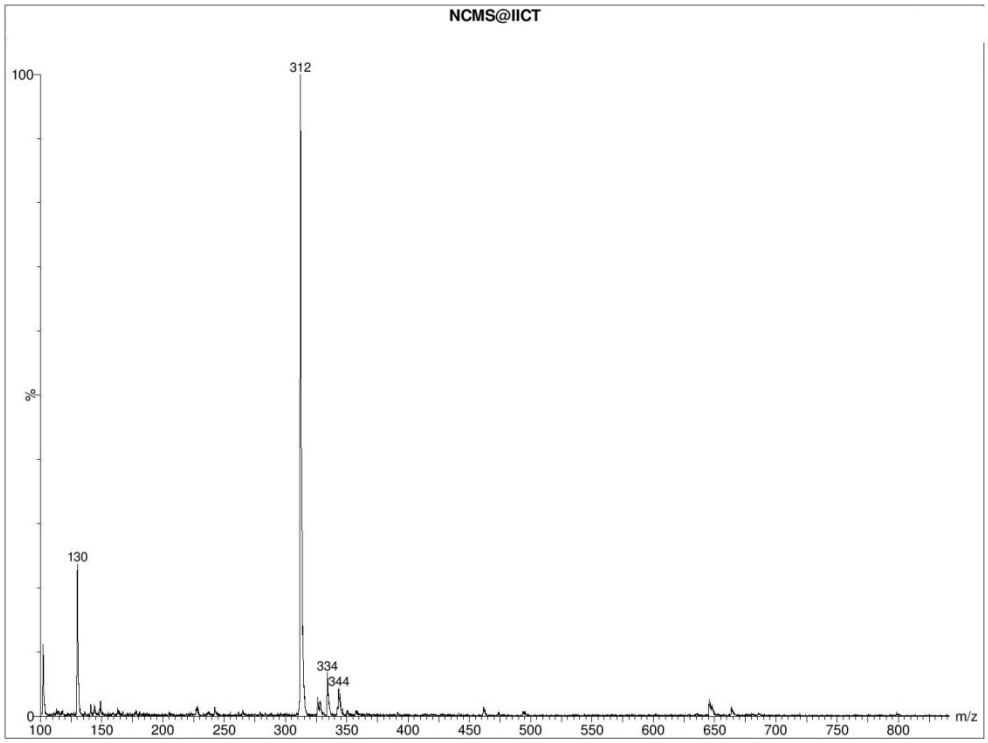

Fig. S8: ESI-Mass spectrum of **10-hexyl-penothiazine-3-carboxaldehyde** (**3**).

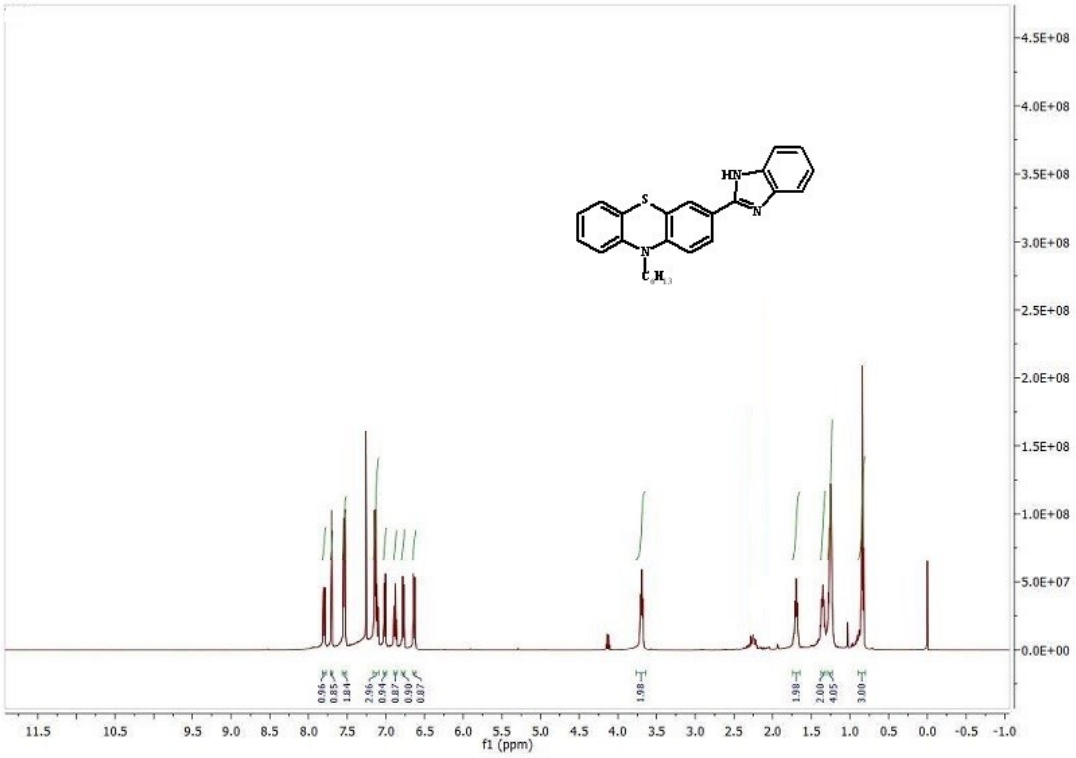

Fig. S9: ^{1}H NMR spectrum of **3-(1H-benzo[d]imidazol-2yl)-10-hexyl-10H-phenothiazine** (**4**) in $CDCl_3$.

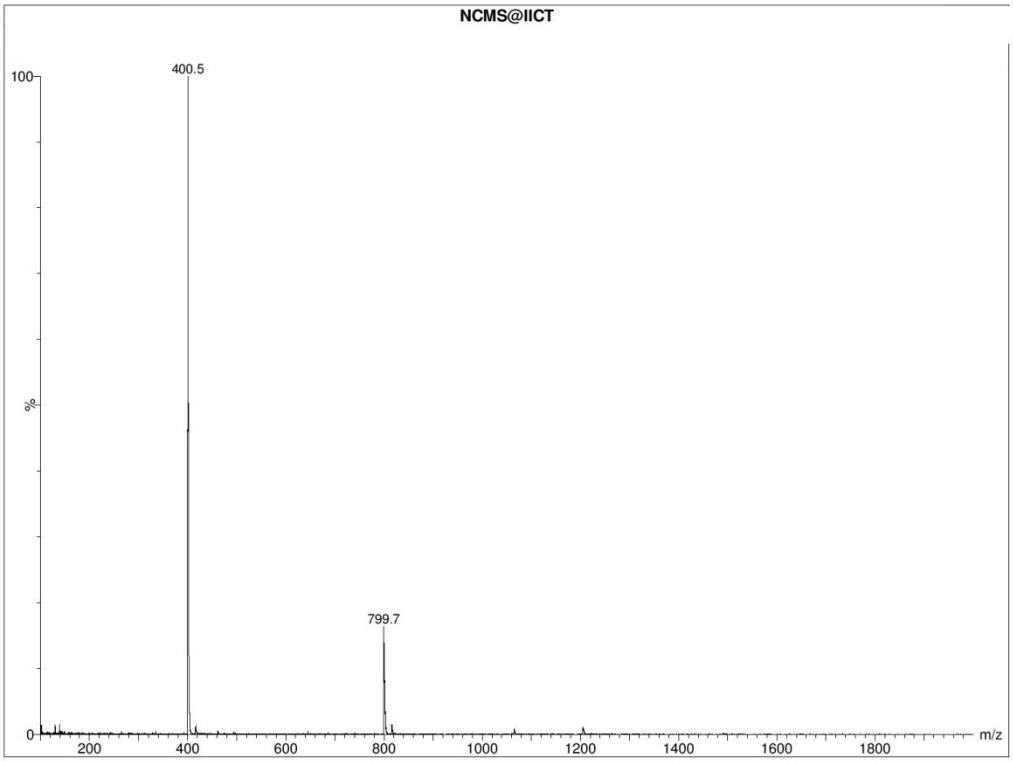

Fig. S10: ESI-Mass spectrum of **3-(1H-benzo[d]imidazol-2yl)-10-hexyl-10H-phenothiazine** (**4**).

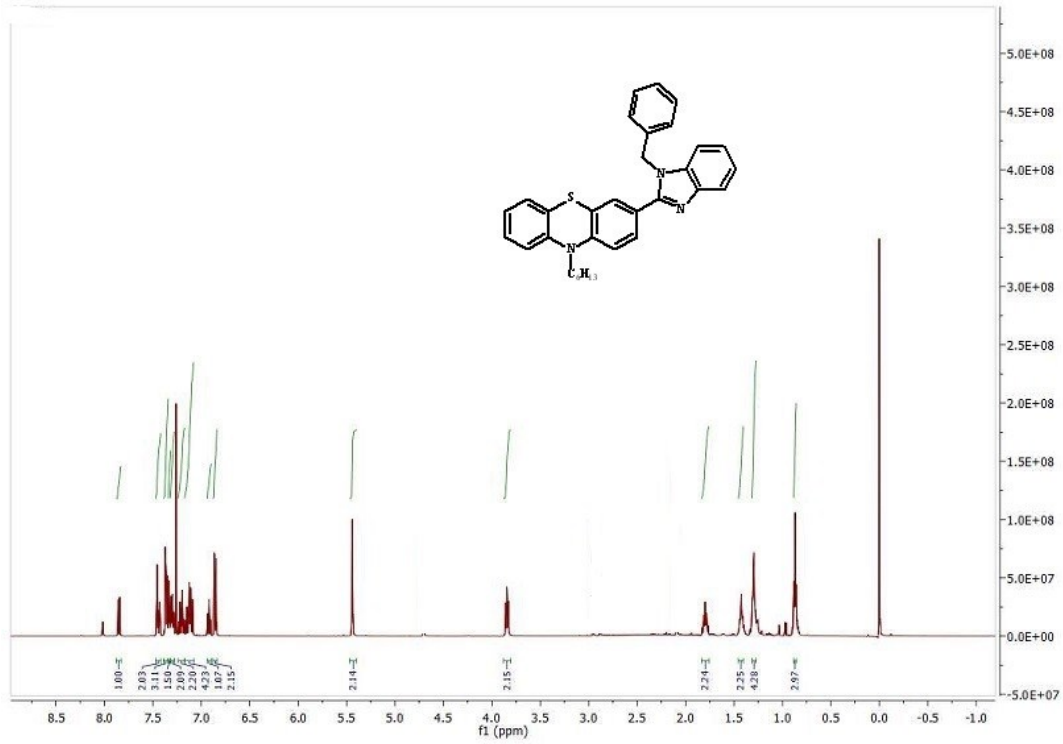

Fig. S11: ^{1}H NMR spectrum of **3-(1H-benzo[d]imidazol-2yl)-10-hexyl-10H-phenothiazine** (**L2**) in $CDCl_3$.

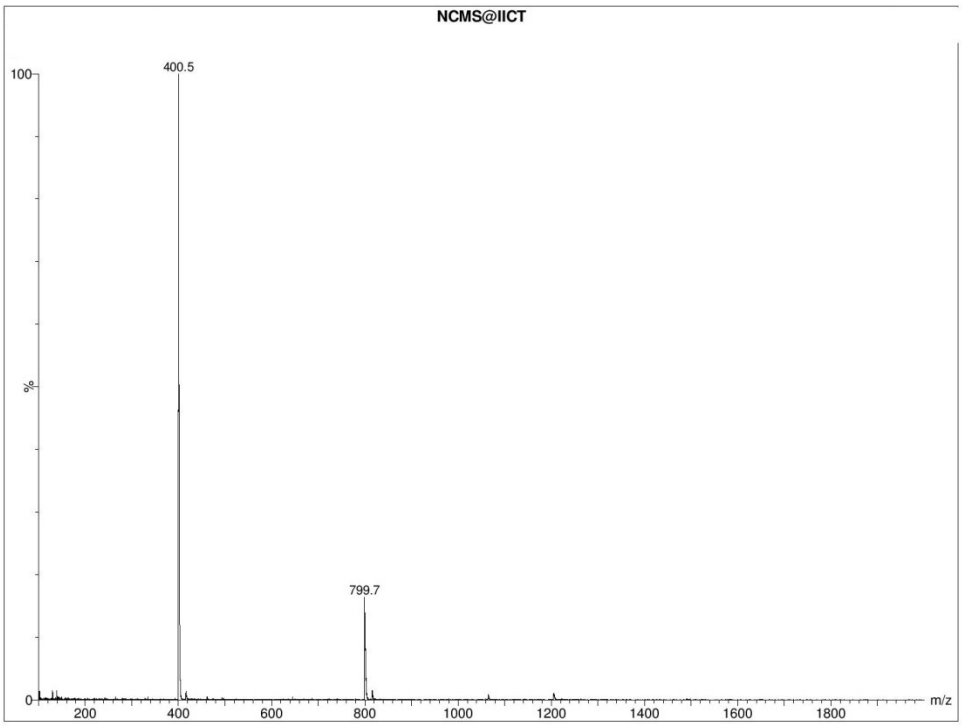

Fig. S12: ESI-Mass spectrum of (**L2**).

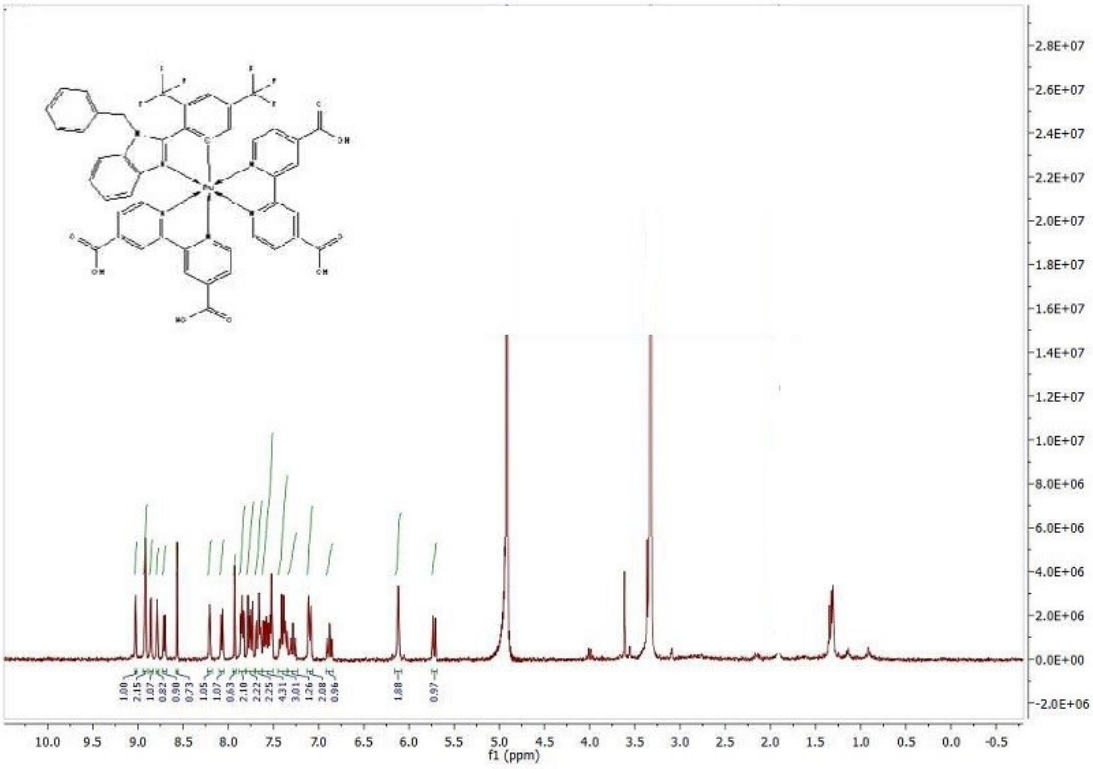

Fig. S13: ^{1}H NMR spectrum of **TC-1** in CD_3OD.

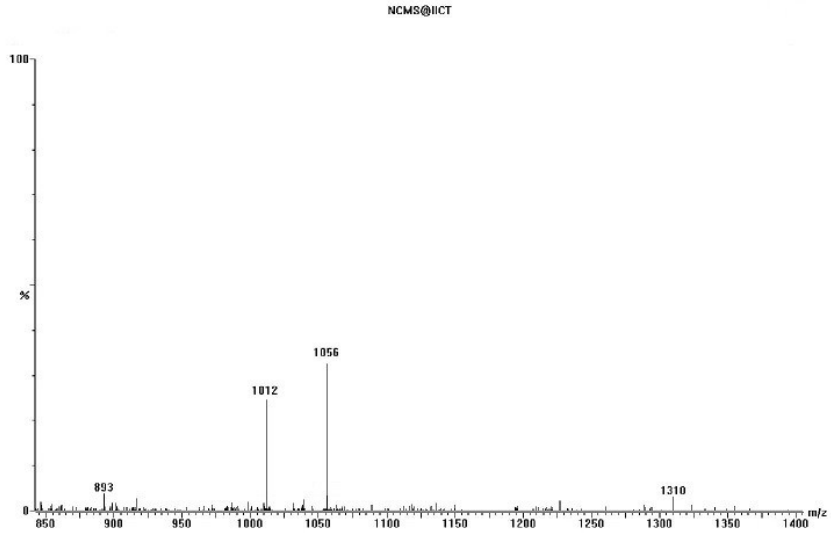

Fig. S14: ESI-Mass spectrum of **TC-1**.

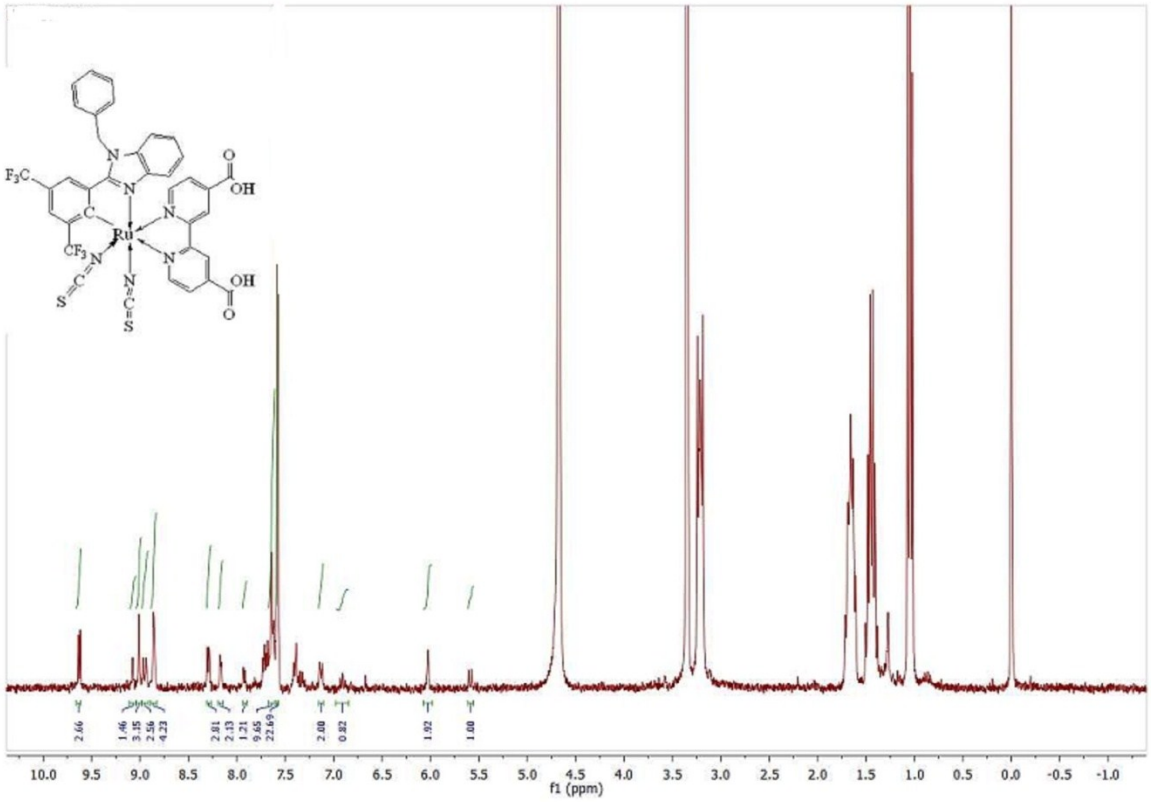

Fig. S15: ^{1}H NMR spectrum of **TC-2** in DMSO-d_6.

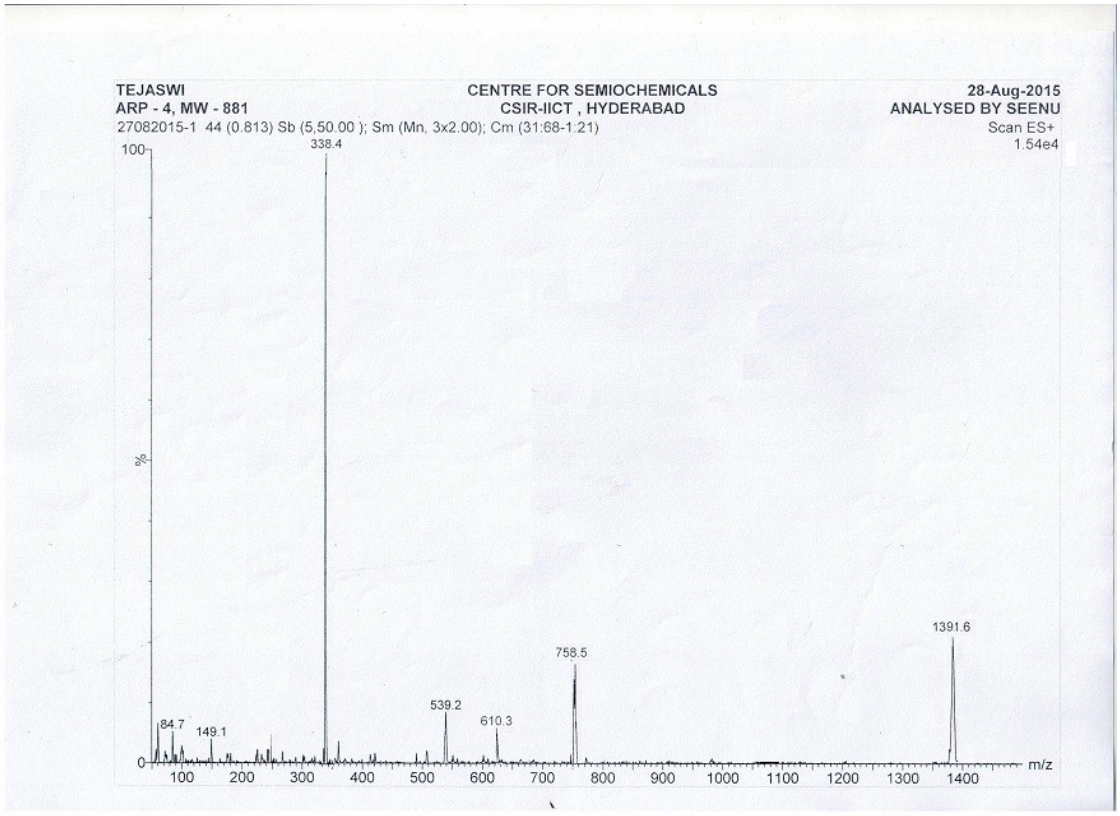

Fig. S16: ESI-Mass spectrum of **TC-2**.

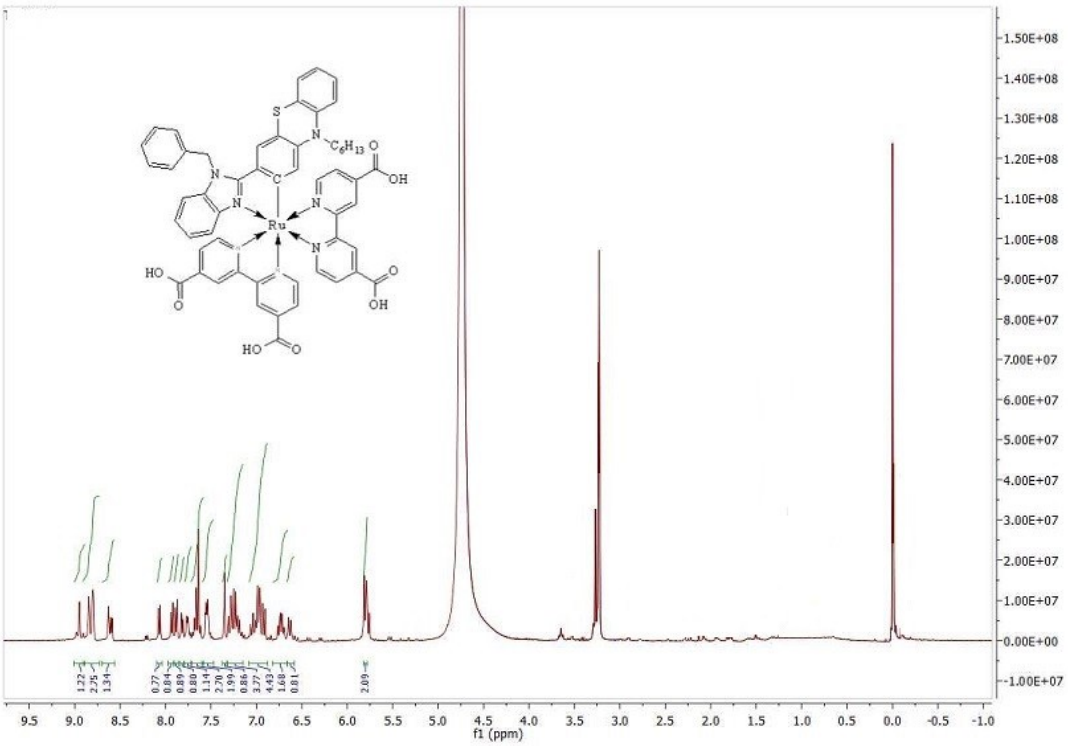

Fig. S17: ^{1}H NMR spectrum of **TC-3** in DMSO-d_6.

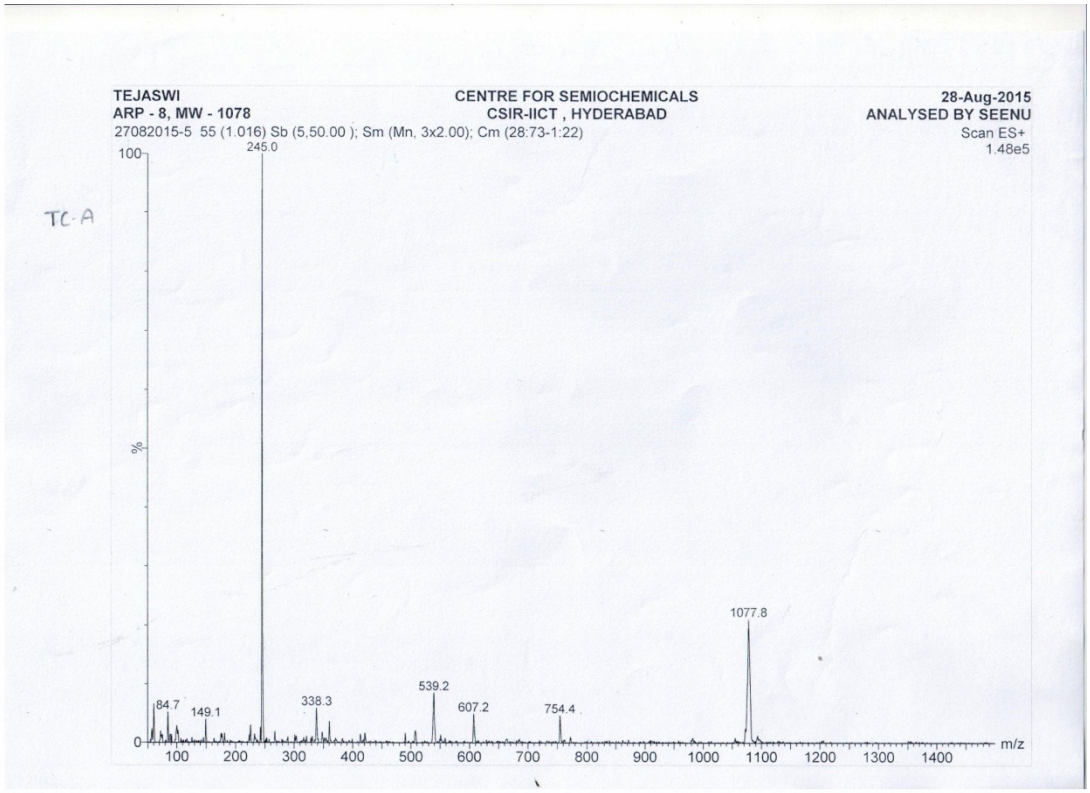

Fig. S18: ESI-Mass spectrum of **TC-3**.

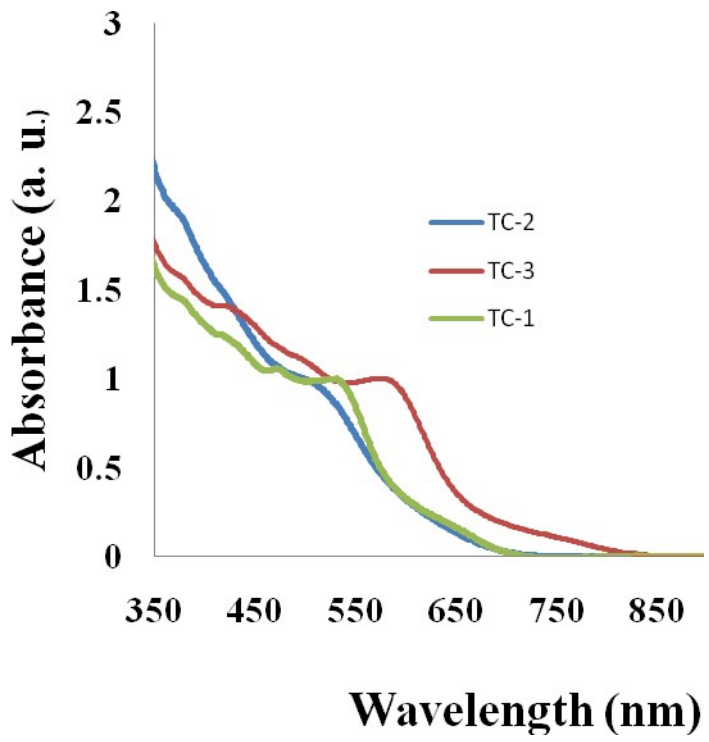

Fig. S19: Absorption spectra of sensitizers adsorbed onto a 6 μm thick TiO_2.

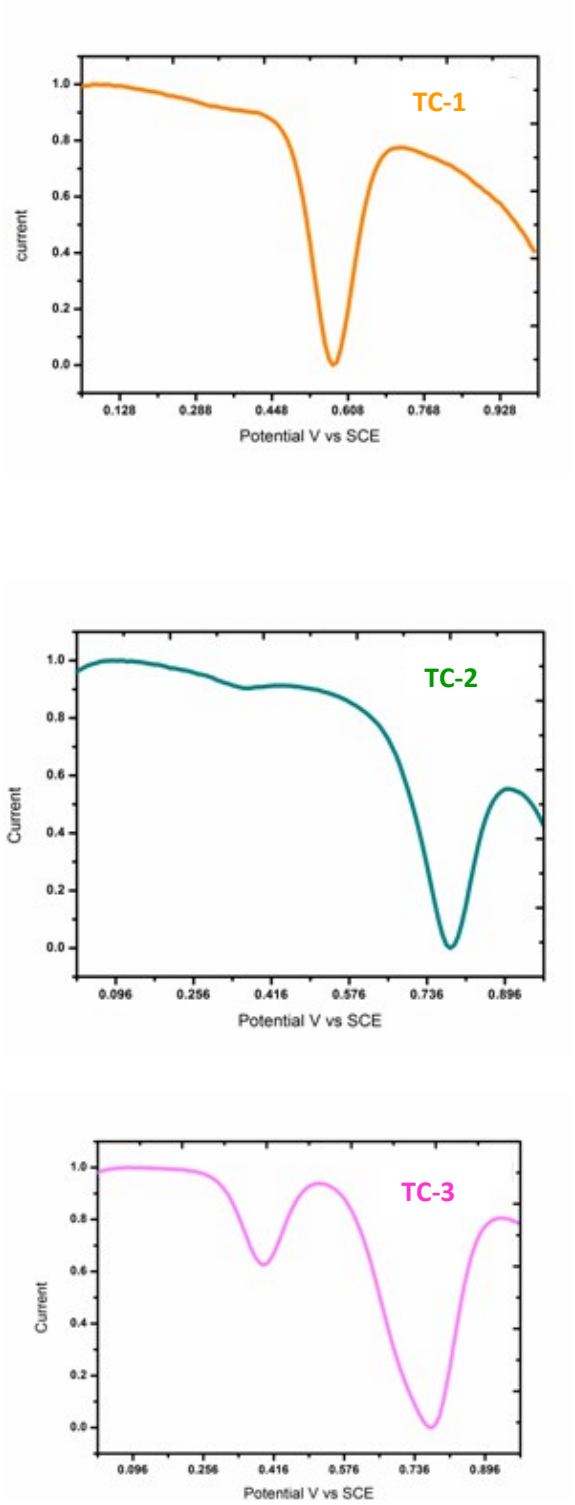

Fig. S20: Differential pulse voltammogramme of complexes **TC-1**, **TC-2** & **TC-3**

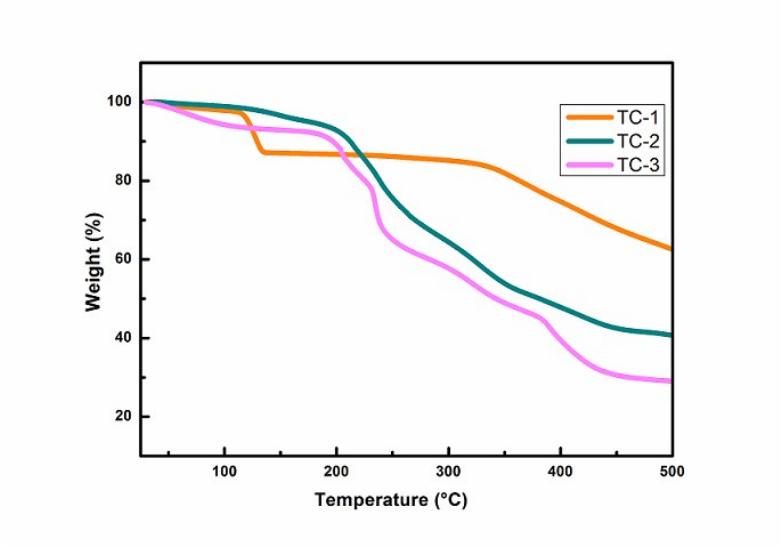

Figure S21: TG/DTG curves of all three heteroleptic complexes with a heating rate of 10 ^{o}C min^{-1} under nitrogen atmosphere.

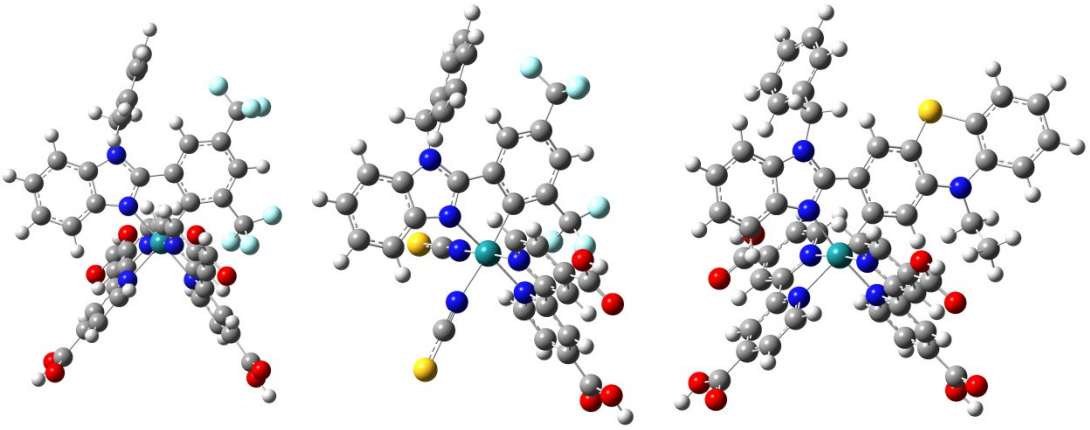

TC-1^{1+} **TC-2**$^{1-}$ **TC-3**$^{1+}$

Figure 22. Optimised Molecular structures of ruthenium complexes.

Table S1. Geometric parameters (in Å and degrees) of Ru complexes at B3LYP/def2-SVP:def2-TZVP-ecp in methanol (Wiberg bond indices shown in parenthesis).

Geometric parameters	**TC-1**$^{1+}$	**TC-2**$^{1-}$	**TC-3**$^{1+}$
Bond lengths (Å)			
Ru-N_1 (NHC)	2.108 (0.53)	2.109 (0.53)	2.114 (0.53)
Ru-N_2 (Bpy/NCS)	2.079 (0.56)	2.056 (0.63)	2.087 (0.56)
Ru-N_3 (trans Bpy/NCS)	2.144 (0.47)	2.126 (0.56)	2.163 (0.45)
Ru-N_4 (Bpy)	2.081 (0.57)	2.053 (0.62)	2.058 (0.59)
Ru-N_5 (cis Bpy)	2.069 (0.57)	2.031 (0.65)	2.055 (0.59)
Ru-C_6 (NHC)	2.117 (0.78)	2.101 (0.82)	2.064 (0.81)
Bond angle (°)			
N_2-Ru-N_3	77.64	88.97	77.10
N_3-Ru-N_4	78.54	79.43	78.97
N_1-Ru-C_6	78.82	79.05	78.43

Table S2. Calculated absorption spectra wavelengths (nm), oscillator strengths (*f*), at TD-CAM-B3LYP/def2-SVP:def2-TZVP-ecp on B3LYP/def2-SVP:def2-TZVP–ecp optimized geometries in methanol solvent using PCM solvation. (the major transition configurations (CI) is given for transitions > 5%)

Molecule	State	eV/nm	Major contribution MOs
TC-1^{1+} + PF_6^-	S5	2.5292/490 (0.1982)	H-2→LUMO (45%), H-1→L+1 (29%), H-2→L+1 (7%), H-1→LUMO (8%), HOMO→LUMO (5%)
	S8	3.1865/389 (0.0645)	HOMO→L+2 (53%), HOMO→L+4 (21%), HOMO→L+5 (12%)
TC-2^{2-}	S1	1.8909/656 (0.0224)	H-2→LUMO (28%), HOMO→LUMO (60%)
	S3	2.3797/521 (0.1657)	H-2→LUMO (59%), HOMO→LUMO (22%), HOMO→L+2 (10%)
	S5	2.8256/438 (0.1098)	H-1→L+1 (28%), HOMO→L+2 (55%)
	S25	4.1681/297 (0.2735)	H-9→L+1 (10%), H-8→LUMO (16%), H-5→L+1 (11%), H-3→L+1 (30%),H-12→LUMO (5%), H-6→L+1 (6%)
TC-2^{2-}+ 2TMA$^+$	S3	2.4269/511 (0.1519)	H-2→LUMO (33%), H-1→LUMO (40%), HOMO→LUMO (10%)
	S8	3.1131/398 (0.1016)	H-1→L+2 (66%), H-2→L+2 (9%), H-1→LUMO (7%), HOMO→L+2 (6%)
TC-1^{1+} + PF_6^-	S1	1.9486/636 (0.0107)	H-1→LUMO (52%), HOMO→LUMO (29%), H-2→LUMO (8%)
	S3	2.2361/554 (0.0164)	H-3→LUMO (40%), H-2→L+1 (30%), HOMO→LUMO (10%), H-2→LUMO (8%)
	S5	2.3767/521 (0.1946)	H-3→LUMO (29%), H-2→L+1 (43%), H-1→LUMO (7%), HOMO→LUMO (5%)

Table S3. Calculated first three triplet excitation energies in eV, using TD-CAM-B3LYP/def2-SVP:def2-TZVP-ecp on B3LYP/def2-SVP:def2-TZVP–ecp optimized geometries in methanol solvent using PCM solvation.

Molecule	CAM-B3LYP Triplet (eV)/nm	Major contribution MOs
TC-1^{1+}	1.8994/653	HOMO→LUMO (27%), HOMO→L+1 (57%)
	1.9652/631	H-2→L+1 (26%), H-1→L+1 (29%), HOMO→LUMO (22%) H-2→LUMO (5%), HOMO→L+1 (9%)
	1.9931/622	H-1→L+1 (35%), HOMO→LUMO (33%), HOMO→L+1 (17%)
TC-2^{1-}	1.3797/899	HOMO→LUMO (81%), H-2→LUMO (8%)
	1.5857/782	H-2→LUMO (77%) H-5→LUMO (9%), HOMO→LUMO (8%)
	1.8313/677	H-1→LUMO (85%), H-6→LUMO (5%)
TC-3^{1+}	1.7227/720	H-3→L+1 (16%), H-1→LUMO (17%), H-1→L+1 (24%), HOMO→L+1 (20%)
	1.7941/691	H-3→L+1 (40%), H-2→LUMO (15%), H-2→L+1 (11%), H-1→L+1 (20%)
	1.8687/663	H-2→LUMO (18%), H-2→L+1 (22%), H-1→LUMO (16%), HOMO→LUMO (17%) H-3→LUMO (5%), H-1→L+1 (7%), HOMO→L+1 (6%)

Table S4. The dominant natural transition orbital pairs for the selected excited singlet states and eigenvalues (λ).

TC-1^{+}	Hole	Electron	λ	Character
S5	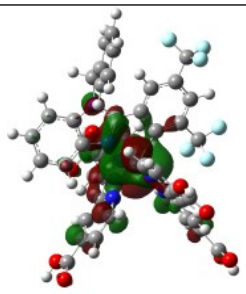	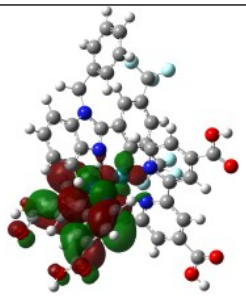	0.56	Ru/C^N→Bpy
	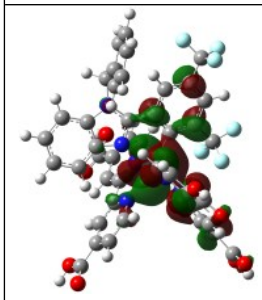	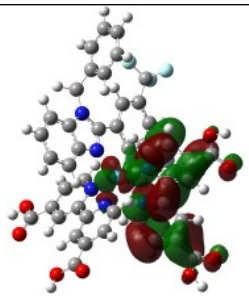	0.42	Ru/C^N→Bpy
S8	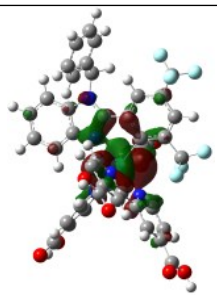	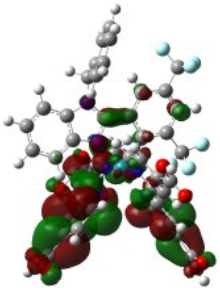	0.98	Ru→Bpy
S30	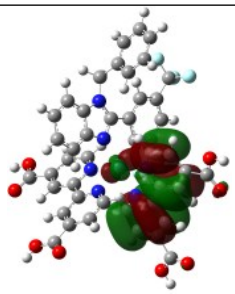	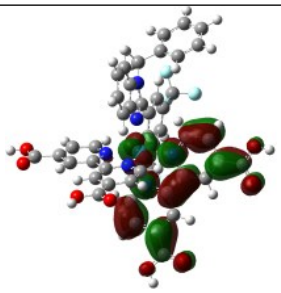	0.53	Bpy→Bpy

	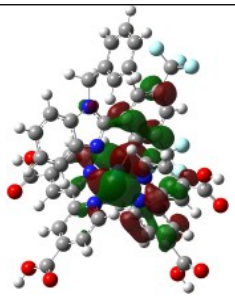	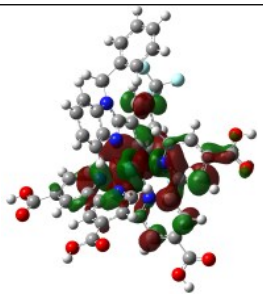	0.22	
	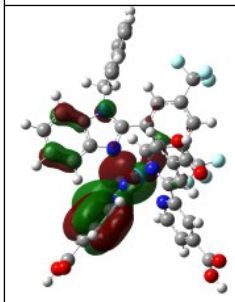	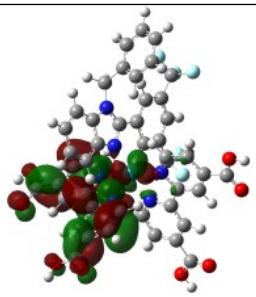	0.13	Bpy→Bpy

TC-2^{-}	Hole	Electron	λ	Character
S1	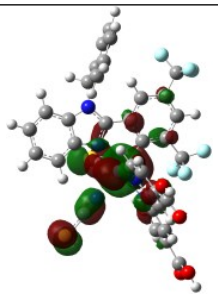	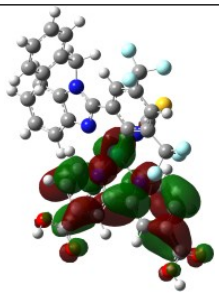	0.99	Ru/NCS→Bpy
S3	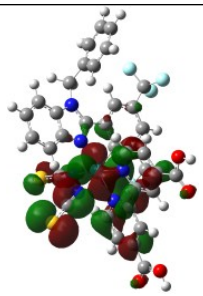	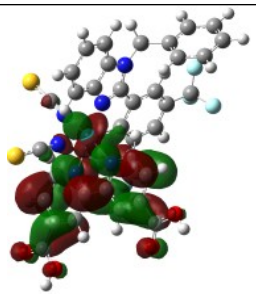	0.82	Ru/NCS→Bpy
	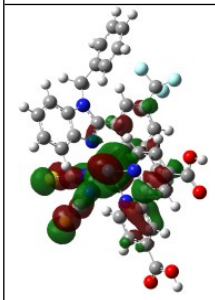	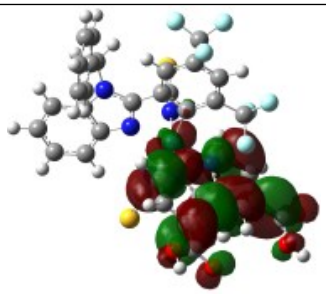	0.17	Ru/NCS→Bpy

S8	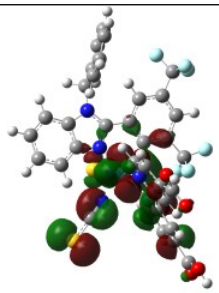	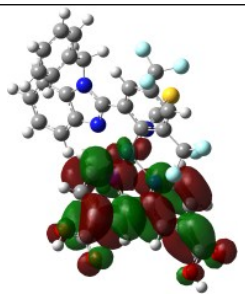	0.70	Ru/NCS→Bpy
	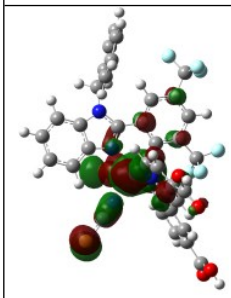	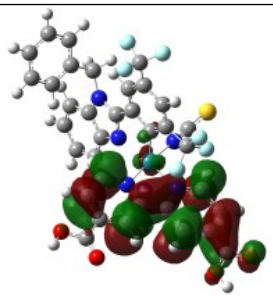	0.24	Ru/NCS→Bpy
S26	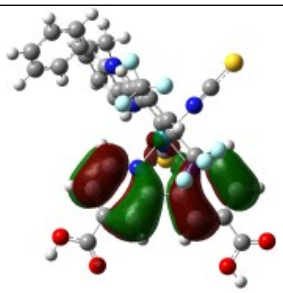	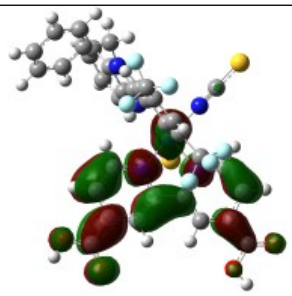	0.50	Bpy→Bpy
	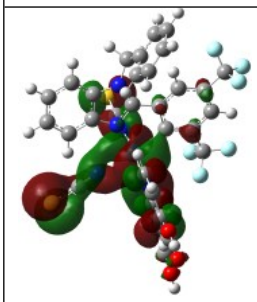		0.23	Ru/NCS→Bpy
	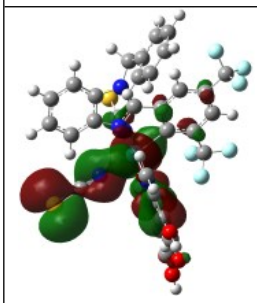	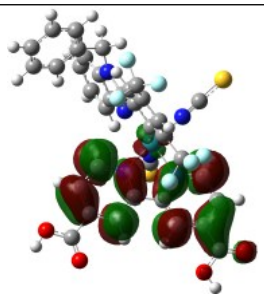	0.17	Ru/NCS→Bpy

TC-3^{+}	Hole	Electron	λ	Character

S3	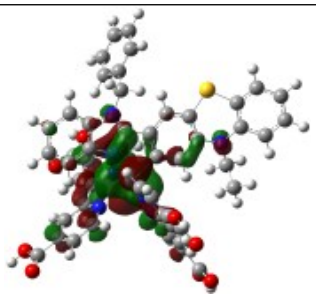	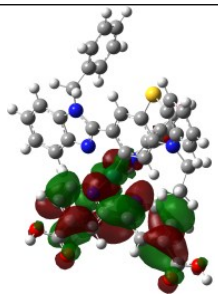	0.82	Ru/C^N→Bpy
	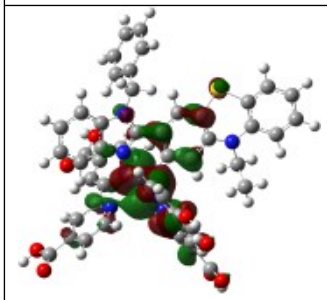	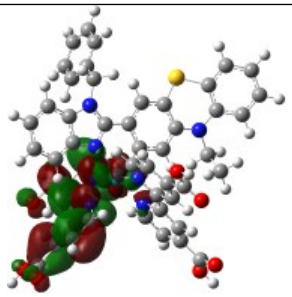	0.17	Ru/C^N→Bpy
S5	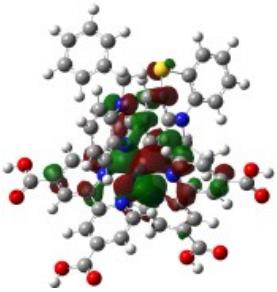	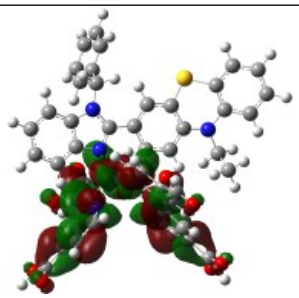	0.66	Ru/C^N→Bpy
	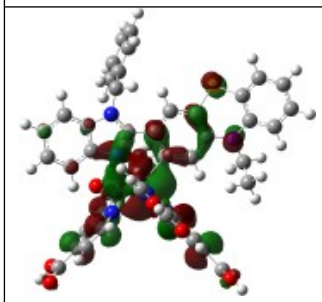	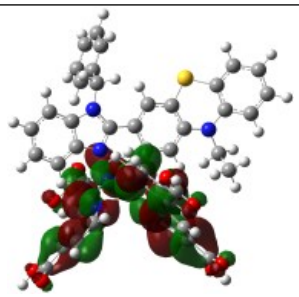	0.32	Ru/C^N→Bpy
S10	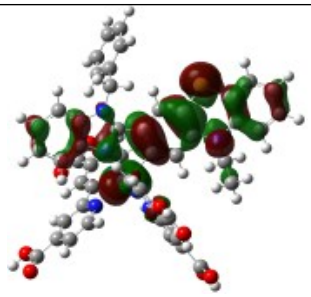	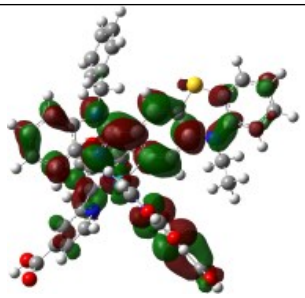	0.77	Ru/C^N→C^N

	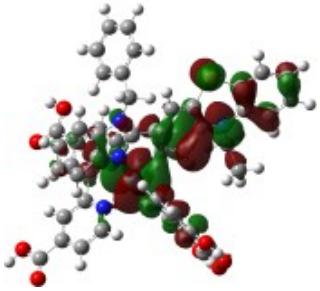	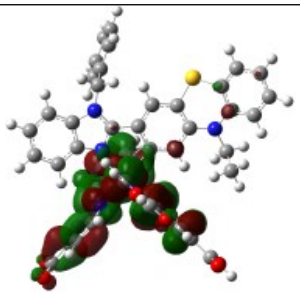	0.19	Ru/C^N→Bpy/Ru
S25	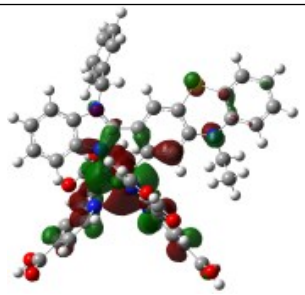	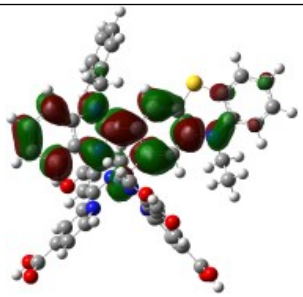	0.82	Ru→C^N
	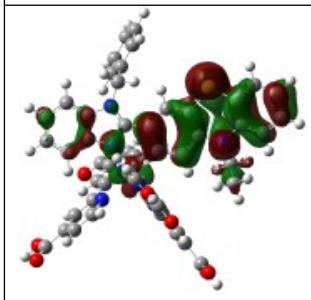	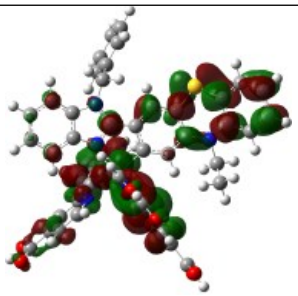	0.15	Ru/C^N→C^N/Bpy